Islamic Azad University

Journal of

Optoelectronical Nanostructures

Spring 2019 / Vol. 4, No. 2

Optoelectronic Properties of PbS Films: Effect of Carrier Gas

Mohsen Cheraghizade[*,1]

[1] Young Researchers and Elite Club, Ahvaz Branch, Islamic Azad University, Ahvaz, Iran

(Received 21 Apr. 2019; Revised 18 May 2019; Accepted 26 May 2019; Published 15 Jun. 2019)

Abstract: In this study, lead sulfide (PbS) films were grown on Fluorine-doped Tin Oxide (FTO) glass substrate by thermal evaporation in a horizontal furnace to investigate carrier gas effect on structural, morphological, elemental, optical, electrical and photovoltaic properties of PbS. X-ray diffraction (XRD) patterns confirmed the formation of cubic polycrystalline PbS particles for all samples. The results showed that using $Ar+H_2$ as a carrier gas increased crystallite size of the film. Field emission scanning electron microscopy (FESEM) images showed nano-dimension surface morphologies and revealed that using carrier gas can make the obtained films and their surface porosities more uniform and regular. Also, the elemental analysis demonstrates that using mixed carrier gas provides a better stoichiometry for PbS film. Optical and electrical evaluations indicated improvements in absorption intensity and electrical conductivity of the PbS film when using the mixed carrier gas. Finally, the deposited films were characterized as solar cells and their quality parameters (QP) were extracted and presented. The obtained results illustrate the improvement in QPs of PbS solar cell when using mixed carrier gas.

Keywords: Lead sulfide (PbS), Thermal evaporation, Carrier gas, Optoelectronic properties, solar cell

1. INTRODUCTION

Today, the role of semiconducting materials is not hidden in the top and efficient technologies. This role has become more important, especially in cases related to serious human problems such as the issues of global pollution and the application of clean and renewable energies [1-4]. In this respect, semiconducting solar cells have gained much popularity among researchers. Usually, semiconductor materials that are used as absorber layers of solar cells have energy band gaps in the range of 1.20 to 2.50 eV [5, 6]. This range of band gap energy is selected because solar rays have the highest intensity in this range

* Corresponding author email: **mohsen.cheraghizade@iauahvaz.ac.ir**

(in term of wavelength) [7]. Lead sulfide (PbS) is a compound semiconductor with an energy band gap that falls in this range. Therefore, it is suitable to use PbS in the fabrication of solar cells. So far, many studies have been reported on using different growth and deposition methods to produce PbS films for solar cells and explore various PbS parameters to enhance the quality of the fabricated films [8-11]. In this regard, our research group has reported two studies about the effect of carrier gas on physical properties of PbS nanostructures deposited by physical vapor deposition (PVD) and chemical vapor deposition (CVD) methods [12, 13]. In the first study, the obtained PbS films showed star- and flower-like surface morphologies with micron- and nano-sized dimensions that could be named PbS mesostructures. X-ray diffraction (XRD) and Raman structural studies indicated that hydrogen gas stream could improve the crystalline quality of PbS film. Furthermore, optical characterization of the PbS films revealed that their optical band gaps are in the infrared (IR) region and hydrogen gas causes a blue shift in their optical band gaps. Therefore, these mesostructures were used for the fabrication of IR detectors. A PbS film with star-shaped morphology can be useful for working with high-speed IR detectors.

In the second study, PbS films were deposited on Pb substrates by CDV method. The Pb sheets used in this research work had two roles: (i) a substrate and (ii) lead (Pb) precursor material. The sulfur powder was used as the sulfur source material. Field emission scanning electron microscopy (FESEM) images showed that hydrogen gas reacting with sulfur, plays a significant role in obtaining different morphologies of PbS nanostructures. The UV-Vis-NIR and PL characterizations exhibited a blue shift in absorption and emission band gap of the PbS film by using hydrogen gas. Bierman et al. reported the CVD-based synthesis of hyperbranched single-crystal PbS nanowires using $PbCl_2$ and S as the precursors to study hydrogen carrier effect [14]. They found that flow rate and duration of hydrogen co-flow in argon carrier gas have considerable impacts on the morphology of the grown PbS particles during the CVD process, from hyperbranched nanowires to micrometer-sized cubes. Moreover, they suggested that elemental Pb, which had been reduced from the vapor by hydrogen, might serve as a vapor-liquid-solid (VLS) catalyst for anisotropic growth of PbS structures. To the best of our knowledge, no study has investigated the influence of hydrogen gas on electrical and photovoltaic properties of PbS films deposited by PVD method. So, in this study, PbS films were deposited through PVD approach on conductive transparent oxide (TCO) substrates and effects of hydrogen gas on structural, morphological, optical, optoelectronic, and photovoltaic properties of the deposited PbS films were investigated. The results show that hydrogen gas improves the efficiency of solar cells fabricated by PbS films.

2. EXPERIMENTAL

Details of the deposition method were reported in our previous works [15]. The differences are that Fluorine-doped Tin Oxide (FTO) glass is used as the substrate here and substrate temperature for all samples was 430 ℃. The FTO substrates were cleaned and prepared for deposition according to the following details. They were washed in an ultrasonication bath for 30 min, at each diluted cleaning solution. The solutions included HCl, NaOH, and ethanol. Finally, the substrates were annealed at 500 ℃ for 30 min. After annealing, the FTO substrates were ready for deposition. The deposition process was carried out at vacuum condition under different carrier gas (Ar and Ar+H_2) following in horizontal furnace. Phase purity investigation of obtained films was carried out by an X-ray diffractometer (XRD; Siefert ID 3003), morphological studies using a field emission scanning electron microscope (FESEM; Hitachi S4160), and elemental analysis of the samples was measured using energy dispersive X-ray system (EDX; Quanta 200F). Optical properties of PbS films were examined using a UV-Vis-NIR spectrometer (Varian Cary 500). For fabrication of photovoltaic devices and electrical characterizations, a proper mask made of a thin aluminum foil was prepared. Au electrodes with thicknesses of ~ 100 nm were deposited on surfaces of the PbS films by a desk sputtering system. Current-voltage (I-V) under darkness and illumination conditions and current density-voltage (J-V) characterizations were recorded by a Keithley source-meter 2400 under standard illumination of solar rays (100 mW cm^{-2}) while these evaluations were carried out by a Solar cell simulator III-200+, Nanosat Co., Iran. The effective area of each sample that was exposed to illumination equaled 0.25 cm^2.

3. RESULTS AND DISCUSSION

Fig. 1 shows XRD patterns of the PbS films and indicates the formation of polycrystalline cubic PbS according to the associated standard XRD card (JCPDS Card No. 00-001-0880) [16]. In this figure, all diffraction peaks are labeled by the relevant miller indices based on standard patterns. It can be observed that using the mixed carrier gas has increased the intensity of the diffraction peaks, suggesting the higher stoichiometry for this sample (hydrogen-assisted). Crystallite size (D) and lattice constant (a) values of the samples can be calculated from the following equations [17]. The obtained results are presented in Table 1.

$$D = \frac{0.94\,\lambda}{\beta\,Cos\theta} \quad (1)$$

$$\frac{1}{d^2} = \frac{h^2 + k^2 + l^2}{a^2} \quad (2)$$

In these equations, λ is X-ray wavelength, β is full width at half maximum (FWHM), θ is the position of the diffraction peak, d is the distance between the

crystalline sheets, and *h*, *k*, and *l* are Miller indices. The obtained results (Table 1) imply that hydrogen flow decreases and increases crystallite sizes and lattice constants of the PbS films, respectively. This result is in agreement with previous works [13-15].

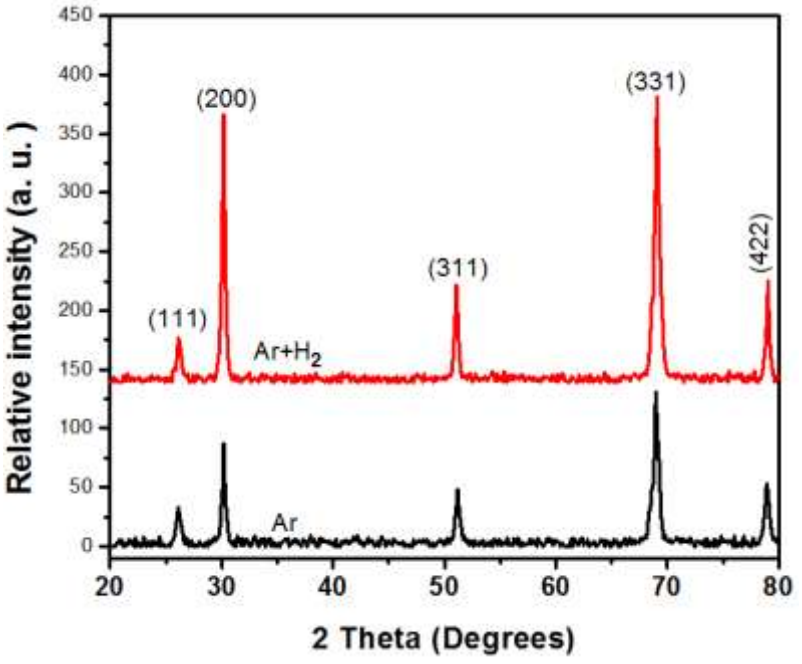

Fig. 1. XRD patterns of PbS films.

TABLE 1. STRUCTURAL PARAMETERS OF PBS FILMS

Sample/Parameters	Crystallite size (nm)	Lattice constant (Å)
Ar	29.36	5.92618
$Ar+H_2$	25.83	5.92684

FESEM images and EDX spectra of the PbS samples are presented in Fig. 2. The images illustrate that relatively uniform films were generated while using hydrogen gas provided more regular and uniform porosities. According to the scale of the images, dimensions of surface morphologies of the PbS films are in the range of nanoparticles. Surface morphology of the sample deposited using Ar carrier gas is a combination of particle and dendrite-like structures whereas surface morphology of the sample deposited by employing the mixed carrier gas

is uniform, particle-like, and with regular porosity. Measurements indicated that using hydrogen gas decreases average diameters of the PbS nanostructures. Furthermore, elemental analysis (EDX) confirmed the existence of Pb and S elements in the films and demonstrated that hydrogen gas yields promoted Pb atomic percentages. The EDX results are indicative of a better stoichiometry and are consistent with the XRD results. With respect to these results, it can be concluded that when the hydrogen carrier gas is used, the atmosphere inside the employed furnace contains hydrogen atoms that are ready to react with sulfur and H_2S forms. This reaction decreases the density of ready sulfur atoms and, as an outcome, more Pb atoms have the opportunity of participating in the reaction for formation of PbS phase that causes the formation of PbS films with higher quality.

Optical absorption and reflectance spectra of the PbS films are presented in Fig. 3a. Maximum absorption is seen in ultra-violet (UV) and visible regions. Clearly, the presence of hydrogen gas increased maximum absorption and reflectance spectra. Also, absorption edges of the samples are in the red region that is the point that the direction of coactivity absorption curve has changed. It is noteworthy that photons with energies equal or higher than the absorption edge energies absorbed by semiconductor films though only photons with energies equal to absorption edge energy have the ability to generate electrical pair carriers (electron/hole). In the energy of a photon is greater than the energy of the absorption edge, then phonon will be generated.

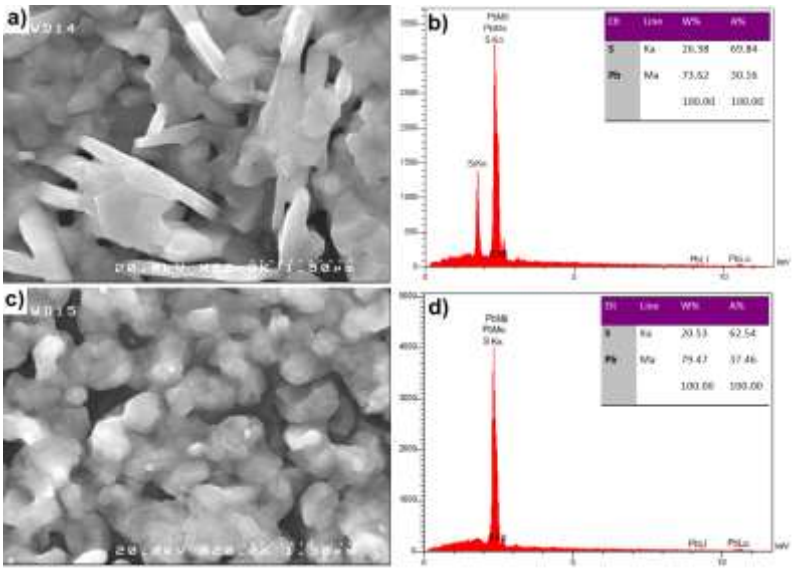

Fig. 2. FESEM images and EDX spectra of PbS films deposited by a, b) Ar and c, d) Ar+H_2 carrier gas.

To evaluate the optical energy band gaps of the PbS films, Tauc plot was used. Tauc plot is founded on Kubelka-Munk model that describes the relationships between absorption and optical energy band gaps of semiconductors [18, 19].

$$(\alpha h\upsilon)^n = A(h\upsilon - E_g) \quad (3)$$

where α is the absorption coefficient, h is Plank's constant, υ is frequency, A is a constant, E_g refers to the optical energy band gap, and n is the characteristic of the transition process. Based on the Tauc plot in Fig. 3b, an increase is seen in the optical energy band gap using hydrogen gas. This observation can be related to the decreased size of the PbS particles according to the surface morphologies depicted in the FESEM images.

For electrical investigations of the PbS films, their current behaviors were studied through applying electrical potential under darkness and illumination condition. Fig. 4 shows the current-voltage (I-V) and V-log(I) curves of the PbS films with non-linear behaviors, which suggests the Schottky nature of the FTO/PbS/Au structures. During the experiments, when hydrogen gas was used at both darkness and illumination states, the turning-on voltage of the device was reduced. Under illumination condition, lower currents were measured for all samples at the same voltages. Such current variations are ascribed to cathodic currents and are characteristics of *p-type* semiconductors [20]. Also, current comparison of the two samples, at the same states of darkness and/or illumination and the same voltages, show higher electrical conductivity (lower electrical resistivity) for the sample deposited under hydrogen gas flow. Based on the literature review, it is seen that increased charge carrier concentration is one of the main factors that enhance the electrical conductivity of similar structures [21, 22].

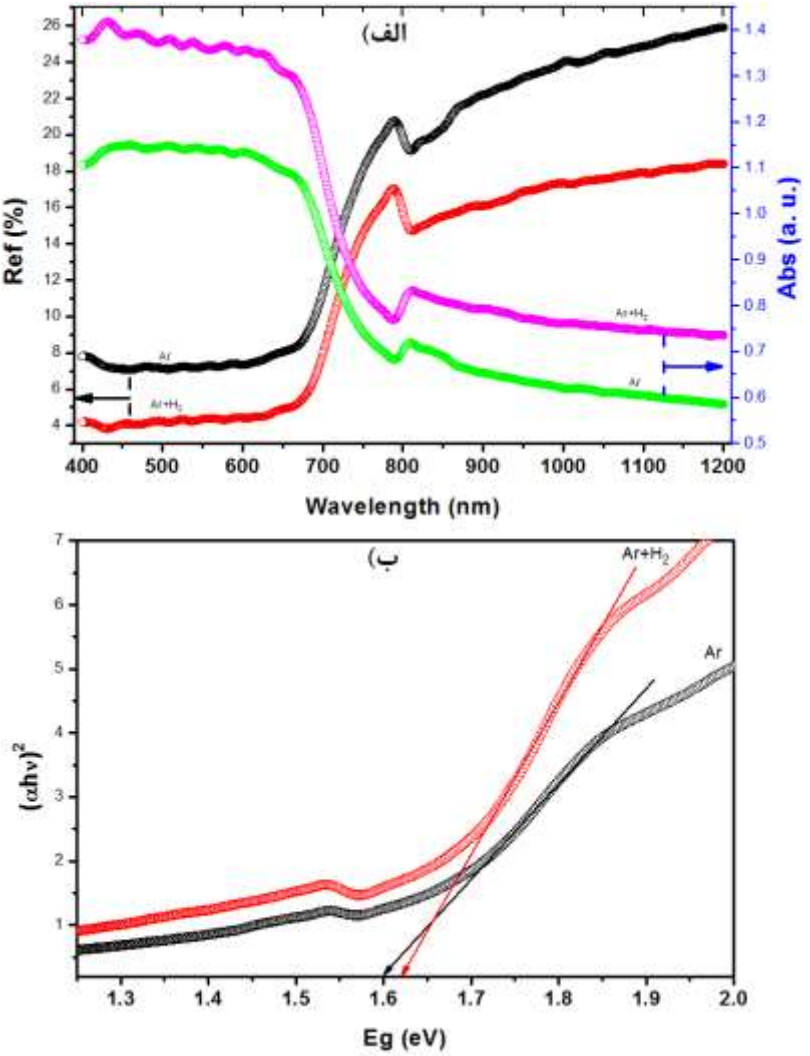

Fig. 3. a) Absorption and reflectance spectra and b) Tauc plot of PbS films.

Based on the linear part of the plots in Figs. 4c and 4d and Eq. 4, ideality factor (*n*) of the junctions formed by the PbS films is calculated as follows [23].

$$I = I_0\left(e^{qv/nkT} - 1\right) \quad (4)$$

where I is forward current, I_0 is reverse saturation current, e is Napier's constant, q is electrical charge, v is forward bias voltage, k is Boltzmann's constant, and T is temperature. Calculation of n can provide useful information about recombination types in junctions. At darkness and illumination states, n coefficients for the sample deposited under Ar flow were 0.88 and 0.66 and for the sample deposited using Ar+H_2 stream n coefficients equaled to 0.54 and

0.55, respectively. All obtained ideality factors are below unity, suggesting that recombination is limited to minor charge carriers [24].

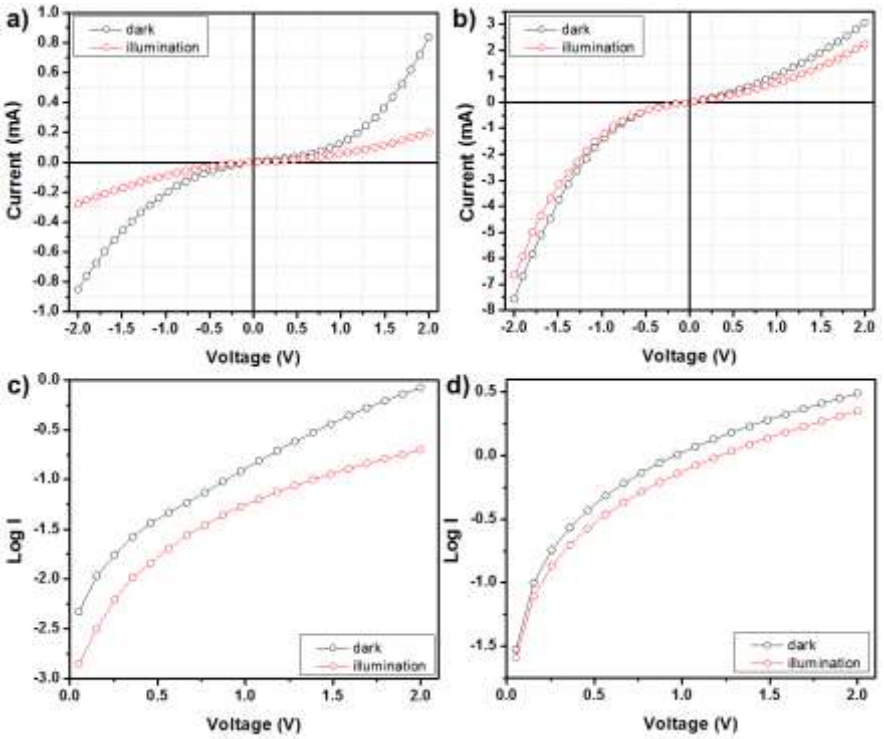

Fig. 4. I-V and logI-V characteristics of PbS films deposited by a, c) Ar and b, d) Ar+H_2 carrier gas in dark and illumination conditions.

J-V curves of the PbS films under 1.5 Air Mass illumination, presented in Fig. 5, were used to investigate their quality parameters in solar cell applications. Solar cell parameters including open-circuit voltage (V_{oc}), short-circuit current (I_{sc}), efficiency (η) fill factor (FF), and series and shunt resistance were calculated through the following equations [25, 26] and summarized in Table 2.

$$\eta = \frac{\frac{V_{oc} \times I_{sc} \times FF}{P_{in}}}{\frac{V_m \times I_m}{}} \times 100 \quad (5)$$

$$FF = \frac{V_{oc} \times I_{sc}}{} \quad (6)$$

$$R_{ss} = \left(\frac{dV}{dI}\right)_{I=0} \quad (7)$$

$$R_{sh} = \left(\frac{dV}{dI}\right)_{V=0} \quad (8)$$

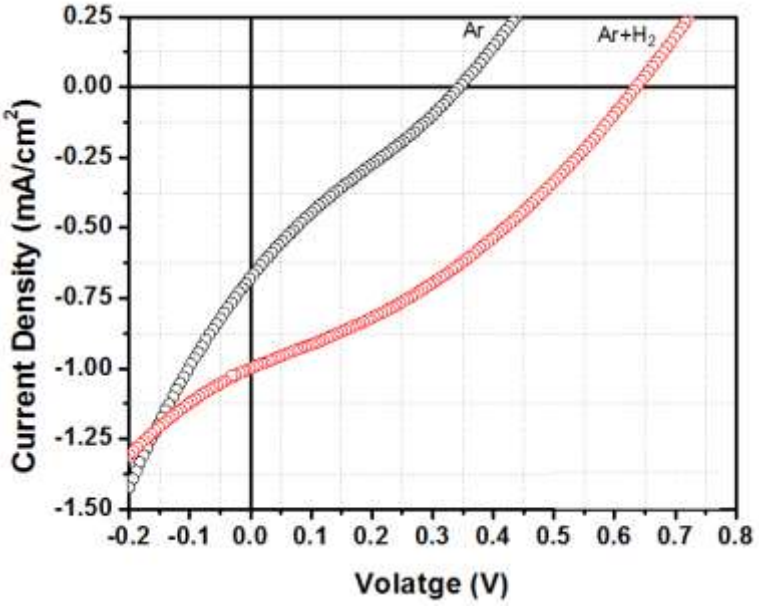

Fig. 5. Solar cell plot of PbS films deposited by different carrier gas.

In these equations, P_{in} is a power of incident solar rays and V_m and I_m are voltage and current characteristics of the points in the fourth quarter at maximum $V_m \times I_m$ (P_m), respectively. The values reported in Table 2 indicate that the efficiency of the solar cell fabricated by employing the PbS films deposited using hydrogen gas is higher than the other sample. According to the obtained results, the improved efficiency of the sample deposited using the mixed carrier gas can be resulted from different factors; e.g., promoted stoichiometry, higher absorption, and improved electrical conductivity.

TABLE 2
QUALITY PARAMETERS OF SOLAR CELL FABRICATED FROM THE PBS FILMS

Sample/Parameters	V_{oc} (V)	J_{sc} (mA/cm^2)	η (%)	FF	R_{ss} (Ω/cm^2)	R_{sh} (Ω/cm^2)
Ar	0.35	0.68	0.06	0.25	1072	315
Ar+H_2	0.64	1.00	0.22	0.22	521	938

4. CONCLUSION

This study investigates carrier gas influences on optoelectronic properties of PbS films as solar cells. XRD patterns and EDX spectra of the films indicated that the presence of hydrogen gas during deposition of PbS film causes the growth of PbS films that are associated with higher stoichiometry due to decreased sulfur vapor density. Furthermore, it was demonstrated that using the mixed carrier gas leads to the increased absorbance intensity and the optical energy band gap of PbS film. Electrical evaluations outlined the *p-type* nature of the PbS films and increased electrical conductivity by applying hydrogen gas due to promoted charge carrier concentration. Ideality factors of all samples were calculated to be less than unity, suggesting that recombination is limited to minor charge carriers. Photovoltaic results exhibited promoted quality parameters of the solar cell device fabricated using the PbS sample deposited under hydrogen gas flow.

ACKNOWLEDGMENT

The author expresses his thanks to Advanced Surface Engineering and Nanomaterials Research Center, Ahvaz Branch, Islamic Azad University, Ahvaz, Iran, for its instrumentation support. Also Author special thanks announced from Dr. Ramin Yousefi and Dr. Farid Jamali-Sheini form Department of Physics, Masjed-Soleiman and Ahvaz Branch, Islamic Azad University, respectively, for their helpful discussions in this research work.

REFERENCES

[1] H. Izadneshan, G. Solookinejad. *Effect of Annealing on Physical Properties of Cu_2ZnSnS_4 (CZTS) Thin Films for Solar Cell Applications*. Journal of Optoelectronical Nanostructures. 3 (2018) 19-28.

[2] F. Jamali-Sheini,M. Cheraghizade,F. Niknia, R. Yousefi. *Enhanced photovoltaic performance of tin sulfide nanoparticles by indium doping*. MRS Communications. 6 (2016) 421-8.

[3] A. Mirkamali, K. Muminov. *The Effect of Change the Thickness on CdS/CdTe Tandem Multi-Junction Solar Cells Efficiency*. Journal of Optoelectronical Nanostructures. 2 (2017) 13-24.

[4] S. M. S. Hashemi Nassab,M. Imanieh, A. Kamaly. *The Effect of Doping and the Thickness of the Layers on CIGS Solar Cell Efficiency*. Journal of Optoelectronical Nanostructures. 1 (2016) 9-24.

[5] J. J. Loferski. *Theoretical Considerations Governing the Choice of the Optimum Semiconductor for Photovoltaic Solar Energy Conversion*. Journal of Applied Physics. 27 (1956) 777-84.

[6] W. Shockley, H. J. Queisser. *Detailed Balance Limit of Efficiency of p-n Junction Solar Cells*. Journal of Applied Physics. 32 (1961) 510-9.

[7] P. Würfel. *Physics of Solar Cells: From Principles to New Concepts*. Wiley, 2008.

[8] A. S. Obaid,M. A. Mahdi,Z. Hassan, M. Bououdina. *Preparation of chemically deposited thin films of CdS/PbS solar cell*. Superlattices and Microstructures. 52 (2012) 816-23.

[9] J. M. Luther,J. Gao,M. T. Lloyd,O. E. Semonin,M. C. Beard, A. J. Nozik. *Stability Assessment on a 3% Bilayer PbS/ZnO Quantum Dot Heterojunction Solar Cell*. Advanced Materials. 22 (2010) 3704-7.

[10] M. Cheraghizade,R. Yousefi, F. Jamali-Sheini. *Substrate Temperature Effect on Photovoltaic Performance of Lead Sulfide (PbS) Nanostructures Deposited by Chemical Vapor Deposition (CVD) method*. Majlesi Journal of Telecommunication Devices. 5 (2016)

[11] C. Justin Raj,S. N. Karthick,S. Park,K. V. Hemalatha,S.-K. Kim,K. Prabakar, et al. *Improved photovoltaic performance of CdSe/CdS/PbS quantum dot sensitized ZnO nanorod array solar cell*. Journal of Power Sources. 248 (2014) 439-46.

[12] M. Cheragizade,R. Yousefi,F. Jamali-Sheini,M. R. Mahmoudian,A. Sa´aedi, N. Ming Huang. *Synthesis and characterization of PbS mesostructures as an IR detector grown by hydrogen-assisted thermal evaporation*. Materials Science in Semiconductor Processing. 26 (2014) 704-9.

[13] R. Yousefi,M. Cheraghizade,F. Jamali-Sheini,W. J. Basirun, N. M. Huang. *Effect of hydrogen gas on the growth process of PbS nanorods grown by a CVD method*. Current Applied Physics. 14 (2014) 1031-5.

[14] M. J. Bierman,Y. K. A. Lau, S. Jin. *Hyperbranched PbS and PbSe Nanowires and the Effect of Hydrogen Gas on Their Synthesis*. Nano Letters. 7 (2007) 2907-12.

[15] M. Cheragizade,R. Yousefi,F. Jamali-Sheini,M. R. Mahmoudian,A. Sa´aedi, N. Ming Huang. *Synthesis and characterization of PbS mesostructures as an IR detector grown by hydrogen-assisted thermal evaporation*. Materials Science in Semiconductor Processing. 26 (2014) 704-9.

[16] P. D. F. ICDD. *International Centre for Diffraction Data*. Powder Diffraction File, Newtown Square, Pennsylvania, USA. (1997)

[17] B. D. Cullity. *Elements of X-Ray Diffraction.* American Journal of Physics. 25 (1957) 394-5.

[18] F. Jamali-Sheini,R. Yousefi,N. Ali Bakr,M. Cheraghizade,M. Sookhakian, N. M. Huang. *Highly efficient photo-degradation of methyl blue and band gap shift of SnS nanoparticles under different sonication frequencies*. Materials Science in Semiconductor Processing. 32 (2015) 172-8.

[19] Z. Dehghani Tafti,M. Borhani Zarandi, H. Amrollahi Bioki. *Thermal Annealing Influence over Optical Properties of Thermally Evaporated SnS/CdS Bilayer Thin Films*. Journal of Optoelectronical Nanostructures. 4 (2019) 87-98.

[20] J. He,H. Lindström,A. Hagfeldt, S.-E. Lindquist. *Dye-Sensitized Nanostructured p-Type Nickel Oxide Film as a Photocathode for a Solar Cell*. The Journal of Physical Chemistry B. 103 (1999) 8940-3.

[21] F. Jamali-Sheini,F. Niknia,M. Cheraghizade,R. Yousefi, M. R. Mahmoudian. *Broad Spectral Response of Se-Doped SnS Nanorods Synthesized through Electrodeposition*. ChemElectroChem. 4 (2017) 1478-86.

[22] M. Cheraghizade,F. Jamali-Sheini, R. Yousefi. *Optical, electrical, and photovoltaic properties of PbS thin films by anionic and cationic dopants*. Applied Physics A. 123 (2017) 390.

[23] M. A. Barote,A. A. Yadav, E. U. Masumdar. *Synthesis, characterization and photoelectrochemical properties of n-CdS thin films*. Physica B: Condensed Matter. 406 (2011) 1865-71.

[24] H. Christiana, B. Stuart. PVeducation.

[25] S. M. Sze, K. K. Ng. *Physics of Semiconductor Devices*. Wiley, 2006.

[26] M. Shirkavand,M. Bavir,A. Fattah,H. R. Alaei, M. H. Tayarani Najaran. *The Construction and Comparison of Dye-Sensitized Solar Cells with Blackberry and N719 Dyes*. Journal of Optoelectronical Nanostructures. 3 (2018) 79-92.